The Detection of Voltage Extreme Points of the Shielded Power Supply Bus under the Ultrashort Pulse Excitation

Rustam R. Gazizov[1], Ruslan R. Gazizov[1] and Timur T. Gazizov[1, 2]
[1]Tomsk State University of Control Systems and Radioelectronics, Tomsk, the Russian Federation
[2]Tomsk State Pedagogical University, Tomsk, the Russian Federation

***Abstract* – The paper investigates the propagation of the ultrashort pulse along the conductors of the power supply (PS) bus with improved design. The common-mode and differential-mode excitations of the 100 V ultrashort pulse were used. Eight propagation ways were considered. The voltage maximum of 13.569 V was obtained with a common-mode excitation, and the voltage minimum (minus 16.683 V) was obtained with differential-mode excitation for 50 Ohm terminations.**

***Index Terms* – Simulation, power supply bus, ultrashort pulse, voltage maximum, voltage minimum, common-mode, differential-mode**

I. INTRODUCTION

DEVELOPMENT OF RADIOELECTRONIC equipment occurs together with the increase of complexity and miniaturization of its components. Computer simulation and investigation of the propagation of ultrashort pulse and electrostatic discharge (ESD) are important for developing the equipment for aviation and space industries in particular. The relevance of investigating the ESD propagation in radioelectronic equipment is shown in [1]. The protection of critically important equipment from the ultrashort pulse with modal filters is shown in [2, 3]. The investigation of the influence of different factors including ultrashort pulses on a satellite performance has been done in [4], [5], and [6]. The propagation of an ultrashort pulse in the C-section with different geometric parameters has been investigated in [7]. The common-mode ESD excitation in the PS bus has been simulated in [8]. Different simulation approaches to different-mode and common-mode excitations are considered in [9]. Therefore, it is important to additionally investigate the performance of the PS bus under the excitation of different signals in order to detect vulnerable places.

The aim of this paper is to investigate the ultrashort pulse propagation under the differential-mode and common-mode excitations along the conductors of the PS bus with a shielding conductor.

II. SIMULATION PARAMETERS

As a research structure we chose a PS bus developed in the research laboratory "Security and Electromagnetic Compatibility of Radioelectronic Equipment". The design of the PS bus was changed during the development, and the bus excitation by different signals was simulated. However, the investigation of common-mode and differential-mode excitations by the ultrashort pulse of the shielded PS bus was not carried out.

The performance of spacecraft elements depend on the failure safety of the PS bus. Therefore, it is necessary to increase the reliability of the PS bus. The development of the improved design of the PS bus is being made in order to reduce the spacecraft mass and to increase of interference immunity of the spacecraft onboard equipment. Two types of the excitation were used during the simulation: common-mode excitation with two sources (U_1 and U_2) of the ultrashort pulse with an amplitude of 100 V and differential-mode excitation with two electromagnetic force sources (U_1 and U_2) of the ultrashort pulse with an amplitude of 100 V and minus 100 V. The rise and fall times of the ultrashort pulse were 1 ns and flat top time was 10 ns. All excitations were relative to shielding conductor being considered at a signal reference. All terminations are resistances of 50 Ohm. The circuit-diagram of the PS bus from Fig. 1 has start points (A_1–A_4) and end points (B_1 and B_2) of signal propagation. The description of eight calculations of voltage waveforms under the differential-mode and common-mode excitations is shown in Table I.

The structure under research consists of the bus (multiconductor transmission line (MCTL) sections 7–12), the end branch conductors (MCTL sections 1, 2, 5, 6, 13, 14, 17 and 18) and central branch conductors (MCTL sections 3, 4, 15 и 16) shown in Fig. 1. The length of MCTL sections 1, 2, 5, 6, 13, 14, 17, 18 is 0.5 m, 3–6 is 0.25 m, 7 and 12 is 0.03 m, 8 and 11 is 0.204 m, 9 and 12 is 0.046 m.

978-1-7281-6846-3/20/$31.00 ©2020 IEEE

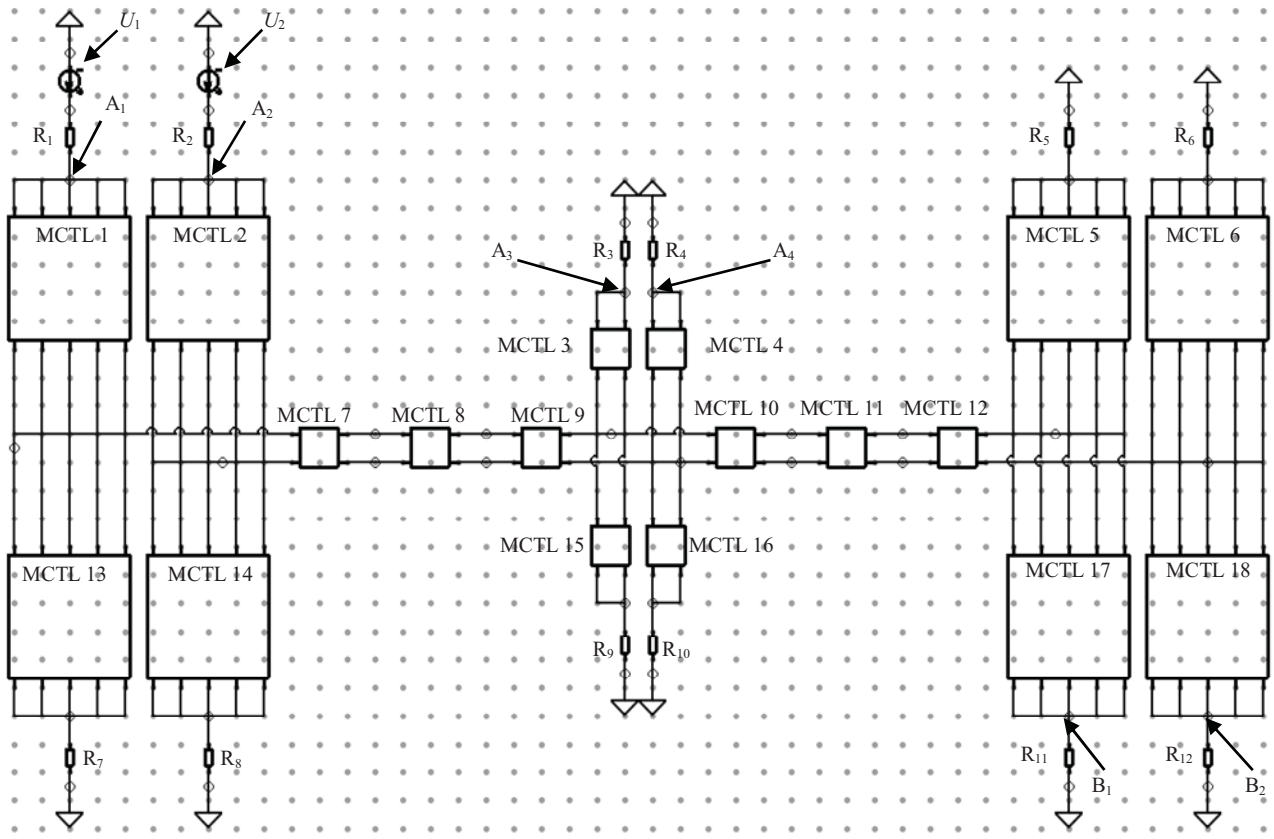

Fig. 1. The circuit diagram of the PS bus.

In order to achieve the required level of accuracy the appropriate segmentation was chosen in all MCTL sections. MCTL sections 1, 2, 5, 6, 13, 14, 17 and 18 are divided into 50 segments; MCTL sections 3, 4, 15 and 16 – into 25 segments; MCTL sections 7 and 12 – into 3 segments; MCTL sections 8 and 11 – into 204 segments; MCTL sections 9 and 10 – into 46 segments. Therefore, the length of each segment in MCTL sections 1–7 and 12–18 is 10 mm and the length of each segment in MCTL sections 8–11 is 1 mm. To investigate the structure, we used the computer simulation software TALGAT [10].

TABLE I
DESCRIPTION OF CALCULATIONS WITH DIFFERENTIAL-MODE AND COMMON-MODE EXCITATIONS

Calculation	Start node (A_i); End node (B_i)
Differential-mode	
1	A_1, B_1
2	A_2, B_2
3	A_3, B_1
4	A_4, B_2
Common-mode	
5	A_1, B_1
6	A_2, B_2
7	A_3, B_1
8	A_4, B_2

The cross-sections of the end and central branches are shown in Fig. 2.

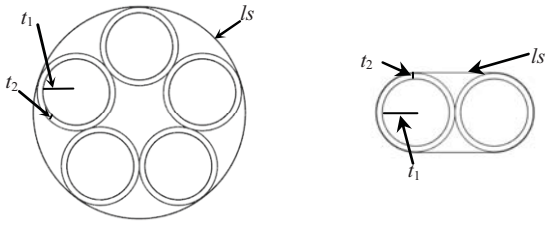

Fig. 2. The cross-sections of the end (*a*) and central (*b*) branch conductors.

The cross-sections of the central (MCTL sections 8–11) and the end parts (MCTL sections 7 and 12) of the PS bus are shown in Fig. 3.

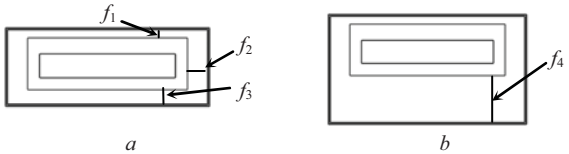

Fig. 3. The cross-sections of the central (*a*) and the end (*b*) parts of the PS bus.

The per-unit-length coefficient matrices of:

- the electromagnetic induction (**L**, nH/m) for the end branch:

$$\mathbf{L}=\begin{bmatrix} 78.76 & 17.61 & 5.64 & 5.61 & 17.56 \\ 17.64 & 78.57 & 17.61 & 5.61 & 5.61 \\ 5.64 & 17.61 & 78.76 & 17.56 & 5.61 \\ 5.61 & 5.61 & 17.56 & 78.51 & 17.52 \\ 17.56 & 5.61 & 5.61 & 17.52 & 78.51 \end{bmatrix}.$$

- the electrostatic induction (**C**, pF/m) for the end branch:

$$\mathbf{C}=\begin{bmatrix} 242.36 & -53.98 & -1.28 & -1.27 & 53.72 \\ -53.99 & 243.46 & -53.99 & -1.26 & -1.26 \\ -1.28 & -53.99 & 242.36 & -53.72 & -1.27 \\ -1.27 & -1.26 & -53.72 & 243.48 & -53.82 \\ -53.72 & -1.26 & -1.27 & -53.82 & 243.48 \end{bmatrix}.$$

- for the central branch, respectively:

$$\mathbf{L}=\begin{bmatrix} 44.1 & 4.76 \\ 4.76 & 44.1 \end{bmatrix} \mathbf{C}=\begin{bmatrix} 448.43 & -49.31 \\ -49.31 & 448.43 \end{bmatrix}.$$

- for the central part of the bus, respectively:

$$\mathbf{L}=\begin{bmatrix} 4.71 & 4.71 \\ 4.71 & 92.88 \end{bmatrix} \mathbf{C}=\begin{bmatrix} 5663.3 & -670.4 \\ -670.4 & 157.4 \end{bmatrix}.$$

- for the end part of the bus, respectively:

$$\mathbf{L}=\begin{bmatrix} 4.22 & 4.22 \\ 4.22 & 110.66 \end{bmatrix} \mathbf{C}=\begin{bmatrix} 5784.06 & -449.29 \\ -449.29 & 106.41 \end{bmatrix}.$$

The geometric parameters of cross-sections (Fig. 2 and 3), are shown in Table II, while the relative dielectric permittivities of isolating materials were taken 2 for wires and 1 for shielding conductor.

TABLE II
GEOMETRIC PARAMETERS OF THE CROSS-SECTIONS

Description	Notation	Value, mm
The radius of the branch conductor	t_1	3
The thickness of the dielectric layer of the branch conductor	t_2	0.5
The thickness of the shielding conductor	ls	0.06
The top thickness of the outside conductor	f_1	1
The thickness side of the outside conductor	f_2	2.5
The bottom thickness of the outside conductor in its short part	f_3	2
The bottom thickness of the outside conductor in its long part	f_4	6

III. SIMULATION RESULTS

For the better understanding, the results of the calculation are shown in Figs. 4, 5 where U_b is the voltage waveform at the input, U_e – at the end, U_{max} – with the highest peak voltage; U_{min} – with the lowest peak voltage. The similar results for other ways of signal propagation with differential-mode and common-mode excitations are shown in Fig. 6, 8, 10 and Fig. 7, 9, 11, 12, respectively. Summary of the results is presented in Tables III and IV.

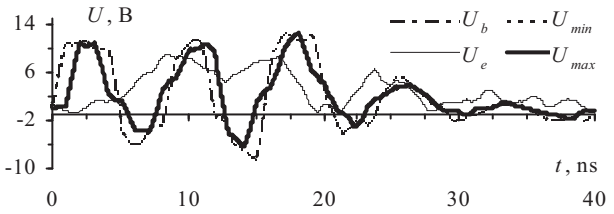

Fig. 4. Voltage waveforms with differential-mode excitation between A_1 to B_1 (calculation 1).

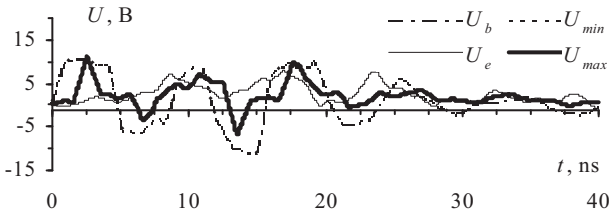

Fig. 5. Voltage waveforms with common-mode excitation between A_1 to B_1 (calculation 5).

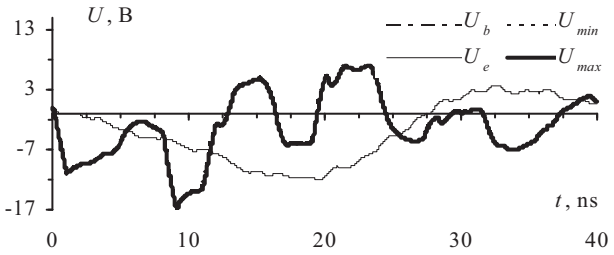

Fig. 6. Voltage waveforms with differential-mode excitation between A_2 to B_2 (calculation 2).

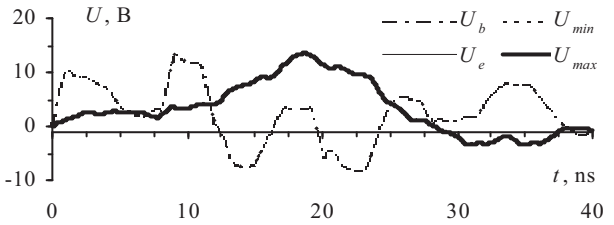

Fig. 7. Voltage waveforms with common-mode excitation between A_2 to B_2 (calculation 6).

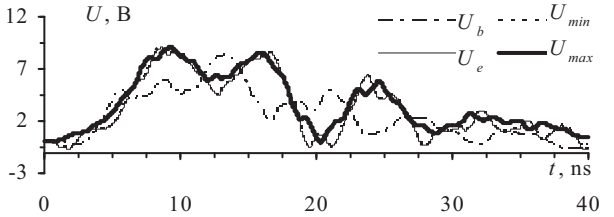

Fig. 8 Voltage waveforms with differential-mode excitation between A_3 to B_1 (calculation 3).

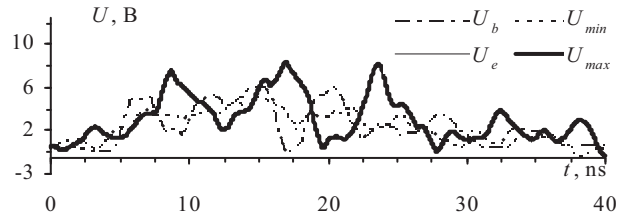

Fig. 9. Voltage waveforms with common-mode excitation between A_3 to B_1 (calculation 7).

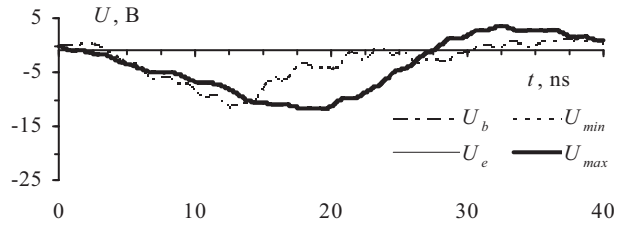

Fig. 10. Voltage waveforms with differential-mode excitation between A_4 to B_2 (calculation 4).

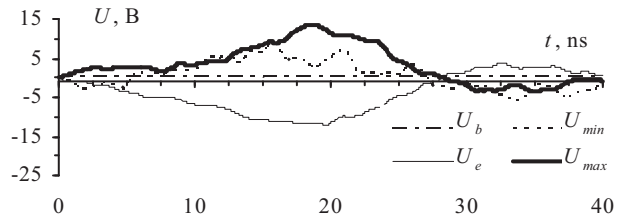

Fig. 11. Voltage waveforms with common-mode excitation between A_4 to B_2 (calculation 8).

TABLE III
SIMULATION RESULTS OF THE SIGNAL PROPAGATION UNDER THE DIFFERENTIAL-MODE EXCITATION

Calc-ulation	MCTL section (segment) for U_{max}	U_{max}, V	MCTL section (segment) for U_{min}	U_{min}, V
1	1 (25)	12.529	1 (1)	–8.607
2	2 (1)	7.074	2 (1)	–16.683
3	17 (31)	9.117	17 (50)	–0.822
4	18 (44)	3.686	18 (50)	–12.086

TABLE IV
SIMULATION RESULTS OF THE SIGNAL PROPAGATION UNDER THE COMMON-MODE EXCITATION

Calc-ulation	MCTL section (segment) for U_{max}	U_{max}, V	MCTL section (segment) for U_{min}	U_{min}, V
5	1 (38)	11.071	1 (1)	–11.355
6	18 (50)	13.569	2 (1)	–8.421
7	17 (50)	7.881	17 (2)	–1.073
8	18 (50)	13.569	11 (116)	–5.983

IV. DISCUSSION OF RESULTS

Consider the results shown in Fig. 4 and 5. The voltage waveforms in both cases are similar and have 3 main voltage maximums from 4 to 12 V with following attenuation. The voltage waveforms in Fig. 6 have 5 peaks of voltage maximum down to 17 V, as opposed to the voltage maximum in Fig. 7, which has smooth form with one voltage extreme point of 15 V with smooth attenuation to 1 V. The voltage maximum waveform from Fig. 8 has 4 signal extreme points with the maximum amplitude of 10 V. The voltage maximum waveform from Fig. 9 has 3 extreme points with the amplitudes around of 8 V. The voltage maximum waveform from Fig. 10 has extreme point with the amplitude of 5 V, while the voltage minimum waveform – minus 10 V. The voltage maximum waveform from Fig. 11 has extreme point 15 V, while minimum – of minus 10 V.

Compare Figs. 4–11. The voltage maximum waveform from Figs. 4–6, 8 and 9 has broken form as opposed to the voltage waveform maximum in Figs. 7, 10, 11. And the voltage minimum waveform from Figs. 4, 5, 8 and 9 has broken form as opposed to the voltage waveform maximum in Figs. 6, 7, 10, 11.

Consider the results of differential-mode excitation which are shown in Table III. The maximum amplitude of the voltage (12.529 V) is obtained when the signal propagated between A_1 to B_1 and the maximum is located in segment 25 of MCTL section 1. The minimum of the voltage (-16.683 V) is obtained when the signal propagated between A_2 to B_2 and the minimum is located in segment 1 of MCTL section 1.

Consider the results of common-mode excitation which are shown in Table IV. The maximum of the voltage (13.569 V) is obtained when the signal propagated between A_2 to B_2 and A_1 to B_2. The maximum is located in segment 50 of MCTL section 18. The minimum of the voltage (minus 11.355 V) is obtained when the signal propagated between A_1 to B_1. The minimum is located in segment 1 of MCTL section 1.

Compare Tables III and IV. The localization segments of the voltage maximums are seen to be similar across the segments of MCTL sections for all calculations, except calculation 2. The localization of the voltage minimums is similar for MCTL sections for all calculations. The localization of the voltage minimums is similar across the segments of MCTL sections for all calculations, except calculations 3 and 7.

Thus, vulnerable point of shielded PS Bus with main voltage maximum (13.569 V) for 6 and 8 calculations with the common-mode excitation under of the ultrashort pulse was obtained. These points are the segment 50 of MCTL section 18. This information will be usefully for the developers of the shielded PS bus, as it is necessary to conduct additional investigation to increase interference immunity of this place.

V. CONCLUSION

The investigation of the ultrashort pulse propagation along conductors of the PS bus in 4 ways under the

common-mode and differential-mode excitations was carried out. The voltage maximum was dedicated under the differential-mode excitation. Meanwhile, for a comprehensive study of the PS bus performance, it is important to make additional investigations of the PS bus with changing the parameters of the excitation signals.

ACKNOWLEDGMENT

This research was funded by the Russian Federation President grant MD-2652.2019.9.

REFERENCES

[1] A. Andersen, J.R. Dennison, and K. Moser, "Perspectives on the Distributions of ESD Breakdowns for Spacecraft Charging Applications," *IEEE Trans. Plasma Sci.*, vol. 45, no. 8, pp. 2031–2035, Jan. 2017.

[2] E.B. Chernikova, A.O. Belousov, T.R. Gazizov, A.M. Zabolotsky, "Using Reflection Symmetry to Improve the Protection of Radio-Electronic Equipment from Ultrashort Pulses", Symmetry, vol. 11, no.7, 25 pages, July, 2019.

[3] E.B. Chernikova, "Ultrashort pulse decomposition in reflection symmetric meander line of four cascaded half-turns / E.B. Chernikova, A.O. Belousov, T.R. Gazizov // IOP Conference Series: Materials Science and Engineering – 2019, vol. 597, no. 1, pp. 1–6, doi: 10.1088/1757-899X/597/1/012067.

[4] D.C. Ferguson, S.P. Worden, and D.E. Hastings, "The space weather threat to situational awareness, communications, and positioning systems," *IEEE Trans. Plasma Sci.*, vol. 43, no. 9, pp. 3086–3098, Sep. 2015.

[5] A.B. Sokolov. "Providing of spacecraft onboard radioelectronic equipment reliability to electrostatic discharge excitation": doctoral diss. Moscow: MIEM, 2009.

[6] E. Tyryshkina. Protection of spacecraft electronics against ESD effects using nanoconductive insulators. 2018 Moscow Workshop on Electronic and Networking Technologies (MWENT), 2018, pp. 1–5, doi:10.1109/mwent.2018.8337174

[7] R. R. Gazizov, A. M. Zabolotsky, T. T. Gazizov, "Research on ultrashort pulse propagation in microstrip C-section with variated separation between coupled conductors," *Dokl. Tom. gos. un-ta system upr. i radioelectroniki*, vol. 19, no. 1, pp. 79–82, 2016. (in Russian)

[8] Ruslan R. Gazizov, Rustam R. Gazizov, T.T. Gazizov, Simulating the influence of electrostatic discharge on a spacecraft power supply bus. International Multi-Conference on Engineering, Computer and Information Sciences (SIBIRCON), 2019, pp 262-272, doi: 10.1109/SIBIRCON48586.2019.8957863.

[9] Yoann Y. Maillet. High-Density Discrete Passive EMI Filter Design for Dc-Fed Motor Drive, Blacksburg, Virginia 2008, P 119.

[10] S.P. Kuksenko, "Preliminary results of TUSUR University project for design of spacecraft power distribution network: EMC simulation" IOP Conference Series: Materials Science and Engineering, 2019, vol. 560, no. 1, pp. 1–6, 10.doi:1088/1757-899X/560/1/012110

Rustam R. Gazizov was born in 1996. He received an Engineering degree from Tomsk State University of Control Systems and Radioelectronics (TUSUR), Tomsk, Russia in 2020. He is the author of 16 scientific papers.

Ruslan R. Gazizov was born in 1993. He received an Engineering degree from TUSUR, Tomsk, Russia in 2016 and a Ph.D. degree in 2018. His is a Junior Research Fellow at TUSUR. R.R. Gazizov is the coauthor of 52 scientific papers.

Timur T. Gazizov was born in 1985. He received an Engineering degree in TUSUR in 2007, a Ph.D. degree in 2008 and a Doctoral degree in 2017. Currently, he is working as a Senior Research Fellow at TUSUR. He is the author and coauthor of 83 scientific papers, including 5 books.